Available online at www.sciencedirect.com
SCIENCE DIRECT®
Bioorganic & Medicinal Chemistry Letters
ELSEVIER
Bioorganic & Medicinal Chemistry Letters 14 (2004) 103–109

3-D-QSAR of *N*-substituted 4-amino-3,3-dialkyl-2(3*H*)-furanone GABA receptor modulators using molecular field analysis and receptor surface modelling study

Nanda Ghoshal[a,*] and Prasenjit K. Mukherjee[b]

[a]*Drug Design, Development and Molecular Modelling Division, Indian Institute of Chemical Biology (CSIR), Kolkata, India*
[b]*Department of Pharmaceutics, Institute of Technology, Bananas Hindu University, Varanasi, India*

Received 22 March 2003; revised 1 October 2003; accepted 5 October 2003

Abstract—We report the theoretical validation of the experimentally observed structure–activity relationships (SAR) of a set of *N*-substituted 4-amino-3,3-dialkyl-2(3*H*)-furanone GABA receptor modulators showing positive allosteric modulatory activity of the $GABA_A$ receptor similar to that shown by Loreclazole. Efforts were made to explain some of the conclusions drawn during this study based on a solitary instance of occurrence of the observation within the dataset. Some of the conclusions selected for study included (i) the enhanced activity for the *R* enantiomer of a compound, (ii) enhanced activity for a compound with an amide type functionality vis-à-vis an amine type functionality at C-4, (iii) enhanced activity for a compound with a carboxamide or carbamate type functionality linking the end group at C-4 over a compound with only the end group attached, provided the alkyl groups attached at C-3 are identical in both cases. The 3-D-QSAR method of molecular field analysis along with receptor–ligand complex stability studies were found to be the most suitable for explaining these activities. While the first conclusion was comprehensively proven, significant support was obtained in case of the latter two. Further comprehensive study is underway and we hope to report them shortly.

1. Introduction

The three dimensional quantitative structure–activity relationship (QSAR) study is a theoretical method for prediction of biological activity based upon its correlation to certain three dimensional structural parameters of the putative drug molecule. The conventional QSAR analysis uses structural (two-dimensional) and other physicochemical parameters to predict the biological activity of an active molecule. Where 3-D-QSAR scores over normal QSAR analysis is in the determination of specific three-dimensional characteristics, which affect the biological activity of the drug molecule, for example stereochemistry of a drug molecule.

The present study is a theoretical verification of a previously conducted study[1] on *N*-substituted 4-amino-3,3-dipropyl-2(3*H*)-furanones showing positive allosteric modulatory activity of the $GABA_A$ receptor similar to that shown by Loreclazole. The study[1] showed that the addition of *N*-carboxamide or *N*-carbamate but not *N*-sulfonyl groups at C-4 position of the 3,3-dialkylbutyrolactone significantly enhances the GABA evoked current potentiation produced by this group of compounds by binding to the Loreclazole allosteric recognition site of the $GABA_A$ receptor. A set of specific conclusions was reached regarding the SAR of this group of compounds. Firstly, the presence of amide type functionality at C-4 produced greater stimulation of GABA currents as compared to an amine type functionality at the same position. The presence of alkyl or dialkyl derivatives at C-3 enhanced the activity of the molecule and in case of monoalkyl or different alkyl groups the *cis* isomer was found to be more active as compared to the *trans* isomer. Furthermore, the biological activity of the molecules were set to reside mainly in the *R* enantiomer of the compound. Finally the carboxamide and carbamate type functionalities at the C-4 were found to produce biological activities of comparable magnitude provided the attached group and alkyl groups at the C-3 position are the same. The studies including radioligand displacement method pointed to the fact that the action was probably being mediated through a new allosteric site—the butyrolactone site at high concentration of the

* Corresponding author. Tel.: +91-33-2473-3491x254; fax: +91-33-2473-0284/5197; e-mail: nghoshal@iicb.res.in

0960-894X/$ - see front matter © 2003 Elsevier Ltd. All rights reserved.
doi:10.1016/j.bmcl.2003.10.006

drug as compared to the picrotoxin site, which is bound by butyrolactones at low concentrations.[1] Two earlier studies[2,3] conducted by Covey et al. showed that the butyrolactones acted through a second putative 'lactone site' and not the picrotoxin site, which was originally taken[4,5] to be the active site. The conclusions[1] reached regarding the SARs of the dataset were mostly based on a single observation concerning two molecules of the dataset except the conclusion drawn on the activity of the sulphur containing compounds. Hence this study was taken up to theoretically validate the observations by studying more molecules of the same group. The suitability of the 3-D-QSAR method of molecular field analysis (MFA) was in the fact that it could differentiate between the *R* and *S* enantiomers of the same compound. Taking to the conclusion that the activity of the molecules was primarily due to the *R* enantiomers, it was decided to build the QSAR equation by assigning the biological activity to the *R* enantiomers of the molecule and later validating on the *S* enantiomers. Since the 3-D data about the receptor site or receptor structure are not available at the moment with the various online resources for example PDB, EMBL, EBI and so on, a receptor surface was modelled on the *R* enantiomers of the original 17 compounds using the experimental biological activity data of these molecules. Following this the energy of interaction (Eint) of these molecules (ligand) with the generated receptor site were calculated to determine the relative stability of the ligand–receptor complex.

2. Molecular field analysis (MFA)[6]

The *Cerius*[2] drug discovery, field calculation, QSAR (MFA) workbenches were utilised for this study. The 17 molecules from the initial dataset were modelled using the 3-D-Sketcher module. The *R* and *S* enantiomers were generated (34 compounds) using the invert bond function of the 3-D-Sketcher module. For all the compounds the conformation space was first scanned using energy optimisation cycles, followed by dynamics simulation using the annealing dynamics. The parameters for the dynamics simulation were Reqtemp—300 K, Dynamic time step—0.01 Ps, Steps—10 000 using constant NVE (constant energy). This was followed by the energy minimisation procedure. The force field used was Universal 1.02 and the molecules were minimised to high convergence using 500 iterations (or more if required) on the smart minimiser.

The butyrolactone moiety was selected as the core model for alignment because it was the largest moiety common to all the structures in the dataset. The alignments of the molecules were conducted using the Common Substructure Search. The models were finally aligned using the Align Strategy-Consensus and the Alignment method-RMS atoms. The RMS consensus was found to be 0.2094.

The field generated was of the rectangular type. The probes used were H^+, OH^-, CH_3. A grid spacing of 2 Å was used and 648 field points were generated. The charge method used was Gasteiger and the energy cutoff was kept at −30 to +30 Kcal. The QSAR equation was generated using the genetic partial least square (G/PLS) method. The number of random equations generated was 300, and 20,000 iterations were run to obtain the equation. The mutation probabilities were set to the system defaults. The genetic preferences were set to defaults of no fixed length, no scaling smoothness of one and the numbers of components were varied. The final result was obtained with the number of components at seven.

The final QSAR equation generated was:

$$\begin{aligned}\text{Biological Activity} = {} & 104.819 \\ & + 0.38187 * \text{'}HO - /557\text{'} \\ & - 3.40695 * \text{'}HO - /261\text{'} \\ & - 6.68673 * \text{'}HO - /323\text{'} \\ & - 0.991745 * \text{'}CH_3/245\text{'} \\ & + 4.02988 * \text{'}CH_3/253\text{'} \\ & - 5.79352 * \text{'}HO - /349\text{'} \\ & + 2.2372 * \text{'}HO - /397\text{'} \\ & + 4.10618 * \text{'}CH_3/343\text{'} \\ & + 3.16438 * \text{'}HO - /542\text{'} \\ & + 7.61204 * \text{'}HO - /423\text{'} \\ & - 0.332004 * \text{'}HO - /541\text{'} \\ & + 0.788757 * \text{ '}HO - /564\text{'} \\ & + 0.958387 * \text{'}H + /461\text{'} \\ & - 7.94293 * \text{'}H + /325\text{'}\end{aligned} \quad (1)$$

where 'HO–/557', 'CH_3/253', 'H+/325'... and so on, are the probes and their numbering (corresponding to spatial positions, shown in Fig. 1) that is, interaction at points 557 by HO–, 253 by CH_3, 325 by H+ respectively. * is the sign of multiplication (all the terms being multiplied by their respective coefficients).

The plot of predicted versus observed activity with the best fit line is shown in Figure 2.

The generalised correlation coefficient $r^2 = 1.000$, cross validated XV$r^2 = 0.922$ and boot strap BS $r^2 = 0.996$.

The number of outliers were four; compounds **2**, **4**, **7**, **13**. Removal of outliers was not considered because firstly the results obtained were good, secondly to keep maximum structural diversity in a small dataset of only 17 compounds under study. Since, as soon as the model looses its structural diversity due to removal of outliers, the predictive power of the model suffers.

The model was validated against the actual biological activity of the *S* enantiomer of compound **5**. The predicted biological activity of the molecule was found to be +82.169 against the experimental biological activity

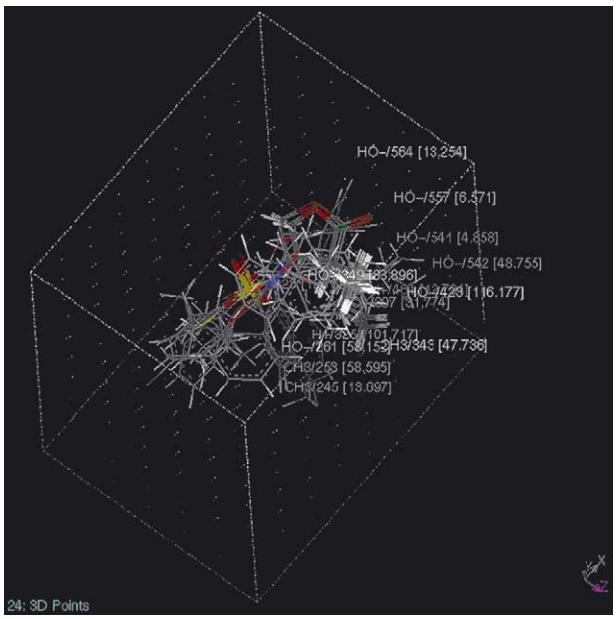

Figure 1. Aligned training set showing the points in 3-D space, used in eq 1.

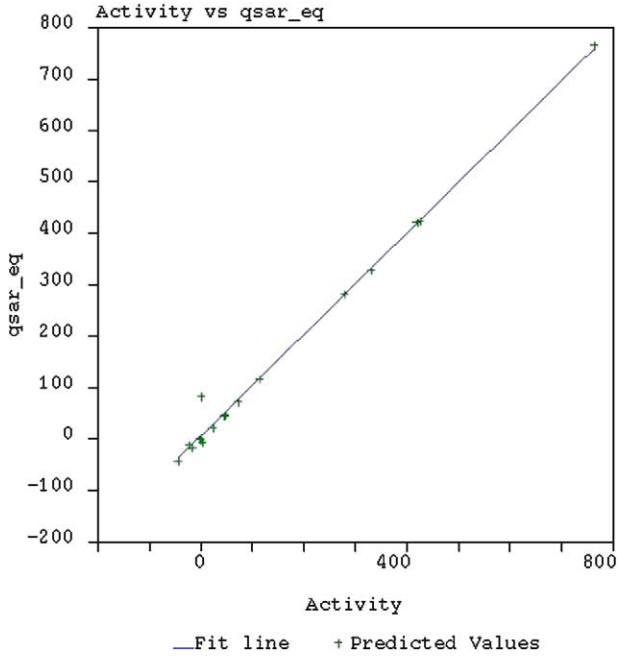

Figure 2. Plot of predicted activity versus observed activity using eq 1.

of 104±4 units. A total of 62 new compounds were designed and modelled for the study in addition to the previously modelled set of 34 compounds (1–17 *R* and *S*). Of the test molecules, the first batch consisted of 66 molecules (58 newly designed and eight previously modelled) using 10 different end groups (*R* and *S*) followed by the carbamate (*R* and *S*) and carboxamide (*R* and *S*) derivative for each, that is six compounds per end group (except sets (**45**, **42**, **5**) and (**49**, **50**, **46**) where the end group is same and substituent at position 3 varies). Apart from this, four compounds [35*RR*(*trans*), 35*SS*(*trans*), 35*RS*(*cis*), 35*SR*(*cis*), vide Table 2] were also modelled to test the *cis*/*trans* variation. The Table 2 features 34 + 66 + 4 = 104 compounds of which the first 34 are modelled while the rest have been designed and modelled for this study (eight of 66 compounds are taken from the first 34-compound set).

3. Receptor surface modelling[6]

The model receptor card of the *Cerius*[2] Drug Discovery (Model Receptor) workbench was used to model the receptor surface. The program offers the use of two forcefields—the Vander Waal and the Wyvill force field. The Wyvill force field was chosen for generating the model because it is less rigid and accommodates for the slight changes in conformation of molecules while calculating the interaction energy (Fig. 3). The biological activity data was utilised while modelling the receptor. Utilising this receptor model the E-interaction, that is the energy of interaction of the receptor–ligand complex was calculated. The model was then validated using the energy terms as descriptors for carrying out a G/PLS analysis.

4. Results and discussion

A ranking system (Table 1) was utilised for classifying the results. Three types of ranking, types 1, 2, 3 based on biological activity, stability of receptor ligand complex, and order of biological activity within a set, respectively, were given to each set of compounds. A set consisted of six compounds, that is the *R* and *S* enantiomers for each of the compound with the end group [2], with the carboxamide derivative [2], with the carbamate derivative [2] at C_4, except the last set which has four compounds. In case of rank types 1 and 2 sub ranking 'A, B, C, D' and 'A, B, C, D, E, F, G', respectively, were given. Each sub ranking referred to a three-letter code referring to the end group, carboxamide and carbamate derivative in that order. The individual letter code is *R* or *S* signifying in case of rank type 1 which enantiomer is more biologically active, in rank type 2 which receptor–ligand complex is more stable. In case of rank type 3 a sub ranking 'A, B, C, D, E, F' was given but here the criteria was the order of biological activity within a set followed by the end group—g, carboxamide—cx, carbamate—ca. The sub-rankings within the individual ranking types are designed to classify the results in terms of their agreement with the experimental conclusions where results classified by rank type 1-A better correlates with the experimental conclusion as compared to rank type 1-D.

The observations (Table 2) regarding the relative activity of the *R* and *S* enantiomers led to a few interesting conclusions. Firstly, for the original dataset of 17 compounds, the calculated values of the *S* enantiomers were less than the *R* enantiomers except for compound **13**. In case of the test molecules the trend of all the *R* enantiomers with greater biological activity was completely

Table 1. Explanation of ranking used in classification of results

Sub ranking	Main ranking type		
	Rank type 1[a] based on biological activity	Rank type 2[b] based on receptor–ligand complex stability	Rank type 3[c] based on biological activity within a set
A	*RRR*	*RRR*	ca > cx > g
B	*SRR*	*SRR*	cx > ca > g
C	*SSR*	*RSR*	cx > g > ca
D	*SSS*	*RRS*	ca > g > cx
E		*RR*[d]	g > cx > ca
F		*SRS*	g > ca > cx
G		*SS*[d]	

[a] *R*(*S*) enantiomer with greater biological activity.
[b] *R*(*S*) enantiomer with greater stability of receptor–ligand complex.
[c] Descending order of biological activity, abbreviations: g, end group; cx, carboxamide; ca, carbamate.
[d] Signifies *R* and *S* receptor–ligand complex equally stable (the more biologically active stereoisomer was considered while ranking).

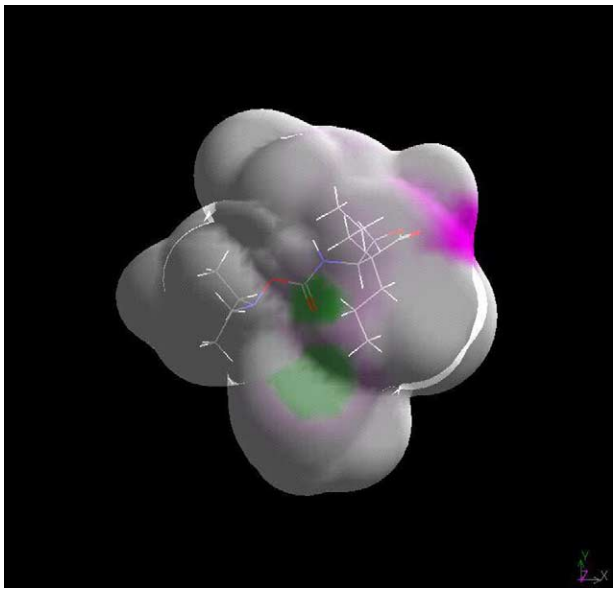

Figure 3. Receptor surface modelled using Wyvill force field.

followed by rank type 1-A (*R*, *R*, *R*). These include the sets (**18**, **28**, **22**), (**39**, **40**, **23**), (**36**, **37**, **7**) and (**43**, **10**, **9**). The trend of two *R* enantiomers showing greater biological activity were found in rank type 1-B (*S*, *R*, *R*), which includes the sets (**33**, **32**, **51**), (**19**, **30**, **31**), (**38**, **34**, **21**) and (**48**, **47**, **20**). The trend of 1 group with greater activity for the *R* enantiomer rank type 1-C were found in the sets (**45**, **42**, **5**) and (**49**, **50**, **46**). The only set with greater activity for the *S* enantiomers was found in rank type 1-D, set (**29**, **27**, **26**).

The observations made on the basis of the interaction energies of the enantiomers with the modelled receptor site pointed towards the greater stability of the receptor–ligand complex formed by the *R* enantiomer. The sets with all the three i.e., end group, carboxamide and carbamate in that order showing greater binding for the *R* enantiomer were found in rank type 2-A (*R*, *R*, *R*). This includes sets (**39**, **40**, **23**), (**29**, **27**, **26**) and (**33**, **32**, **51**). The trend of two groups showing greater stability of the complex formed by the *R* enantiomer were shown by rank type 2-B (*S*, *R*, *R*), sets (**18**, **28**, **22**), (**45**, **42**, **5**), rank type 2-C (*R*, *S*, *R*) set (**19**, **30**, **31**) and rank type 2-D (*R*, *R*, *S*), sets (**36**, **37**, **7**), (**38**, **34**, **21**) and rank type 2-E (—, *R*, *R*), set (**48**, **47**, **20**). The compounds with two groups showing greater stability of the complex with *S* enantiomer were shown by rank type 2-F (*S*, *R*, *S*), set (**49**, **50**, **46**) and rank type 2-G (*S*, *S*,—), set (**43**, **10**, **9**). The findings point towards the fact that the *R* enantiomer is generally the more active of the two enantiomers.

The compounds showing rank type 3-A (ca > cx > g) and rank type 3-B (cx > ca > g) clearly supported the fact that the amine type functionality 'g' was less active as compared to the carboxamide and carbamate derivatives in case of particular end groups. These compounds include rank type 3-A (ca > cx > g), sets (**18**, **28**, **22**), (**33**, **32**, **51**), (**48**, **47**, **20**), (**45**, **42**, **5**), and rank type 3-B (cx > ca > g), set (**43**, **10**, **9**). However, in certain cases like rank type 3-C (cx > g > ca), sets (**39**, **40**, **23**), (**29**, **27**, **26**) and rank type 3-D (ca > g > cx), sets (**38**, **34**, **21**), (**36**, **37**, **7**) the trend was partially followed. In case of rank type 3-E (g > cx > ca), set (**19**, **30**, **31**) and rank type 3-F (g > ca > cx), set(**49**, **50**, **46**) the end group showed higher activity as compared to the amide type functionality and is opposite to the trend, experimentally observed. The activities of the carbamate and the carboxamide derivatives were found to be of the same order in some of the cases.[7] In addition, the range of the CLOGP value for the active compounds fell between 2.5 and 4.05 for the most active compounds (experimental biological activity above 100) except compounds **8**#, **15**# and **16**# (vide Table 2). Although the receptor model validation as shown by the correlation coefficient obtained was not very satisfactory, it has been kept as it is showing the trend observed experimentally. A more comprehensive study is under way.

The activities of the sulphur containing compounds were not evaluated as the six compounds in the experimental dataset supporting low activity of these compounds. The addition of allyl groups at the 3-position in compounds (**49**, **50**, **46**) did not increase the activity of

Table 2. Results obtained from the MFA and receptor–ligand complex stability studies

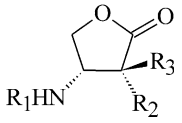

S. no.	R1	R2	R3	Exp BA	Cal BA	CLOGP	Eint	Rank1[a]	Rank2[a]	Rank3[a]
1[e]	Bn	H	H	0		1.261	−2.6			
2[e]	Bn	Allyl	H	73		2.354	−3.1			
3[e]	Bn	H	Allyl	−1		2.354	−2.6			
4[e]	Bn	Allyl	Allyl	115		3.447	−2.7			
5[b]	CO_2Bn	Propyl	Propyl	279		4.01	−3.7			
6[e]	CO_2Et	Propyl	Propyl	426		3.322	−3.1			
7[e]	CO_2allyl	Propyl	Propyl	765		3.567	−2.5			
8[e]	CO_2*t*Bu	Propyl	Propyl	46		4.03	−2.9			
9[e]	CO_2Ph	Propyl	Propyl	330		4.01	−3.1			
10[e]	COPh	Propyl	Propyl	420		3.821	−2.7			
11[e]	SO_2Ph*p*Cl	Propyl	Propyl	23		4.869	−3.4			
12[e]	SO_2Ph*p*OMe	Propyl	Propyl	−22		4.131	−3.2			
13[e]	SO_2Ph*p*CF_3	Propyl	Propyl	−44		5.266	−3.4			
14[e]	$SO_2$2-napthyl	Propyl	Propyl	4		5.027	−3.5			
15[e]	$SO_2$2-thiophene	Propyl	Propyl	−16		3.768	−3			
16[e]	SO_2NMe_2	Propyl	Propyl	−1		2.679	−3			
17[e]	CO_2Bn	H	H	47		1.315	−3			
1*S*	Bn	H	H		−143.46		−1.4			
2*S*	Bn	Allyl	H		−130.79		−2.6			
3*S*	Bn	H	Allyl		−151.07		−2.8			
4*S*	Bn	Allyl	Allyl		9.201		−0.1			
5*S*[c]	CO_2Bn	Propyl	Propyl	104	82.169		−2.4			
6*S*	CO_2Et	Propyl	Propyl		297.372		−2.8			
7*S*	CO_2Allyl	Propyl	Propyl		−13.15		−2.8			
8*S*	CO_2*t*Bu	Propyl	Propyl		−223.82		−2.9			
9*S*	CO_2Ph	Propyl	Propyl		321.457		−3.1			
10*S*	COPh	Propyl	Propyl		−248.94		−3			
11*S*	SO_2 Ph*p*Cl	Propyl	Propyl		−438.55		−3.6			
12*S*	SO_2Ph*p*OMe	Propyl	Propyl		−98.312		−2.8			
13*S*	SO_2Ph*p*CF_3	Propyl	Propyl		−18.79		−3			
14*S*	$SO_2$2-napthyl	Propyl	Propyl		−116.41		−3.4			
15*S*	$SO_2$2-thiophene	Propyl	Propyl		−190.48		−3			
16*S*	SO_2NMe_2	Propyl	Propyl		−437.59		−3.1			
17*S*	CO_2Bn	H	H		29.319		−1.3			
18*R*	$N(CH_3)2$	Propyl	Propyl		208.903		−2.2	A	B	A
18*S*	$N(CH_3)2$	Propyl	Propyl		104.588		−2.7			
28*R*	$C(=O)N(CH_3)_2$	Propyl	Propyl		266.034		−2.99			
28*S*	$C(=O)N(CH_3)_2$	Propyl	Propyl		−314.15		127.53			
22*R*	$C(=O)ON(CH_3)_2$	Propyl	Propyl		400.457		−2.66			
22*S*	$C(=O)ON(CH_3)_2$	Propyl	Propyl		−35.635		7807.56			
39*R*	$N(CH_2CH_3)_2$	Propyl	Propyl		244.18		−2.75	A	A	C
39*S*	$N(CH_2CH_3)_2$	Propyl	Propyl		−449.62		977.89			
40*R*	$C(=O)N(CH_2CH_3)_2$	Propyl	Propyl		292.28		−2.99			
40*S*	$C(=O)N(CH_2CH_3)_2$	Propyl	Propyl		−441.28		127.53			
23*R*	$C(=O)O(CH_2CH_3)_2$	Propyl	Propyl		183.942		32.74			
23*S*	$C(=O)O(CH_2CH_3)_2$	Propyl	Propyl		−423.97		50,951			
29*R*	$C(CH_3)_3$	Propyl	Propyl		96.348		−1.83	D	A	C
29*S*	$C(CH_3)_3$	Propyl	Propyl		111.56		449.89			
27*R*	$C(=O)C(CH_3)_3$	Propyl	Propyl		40.13		−2.68			
27*S*	$C(=O)C(CH_3)_3$	Propyl	Propyl		120.677		3,953,131			
26*R*	$C(=O)OC(CH_3)_3$	Propyl	Propyl		−84.035		−1.16			
26*S*	$C(=O)OC(CH_3)_3$	Propyl	Propyl		−44.518		—[d]			
33*R*	$CH(CH_3)_2$	Propyl	Propyl		−25.766		−2.62	B	A	A
33*S*	$CH(CH_3)_2$	Propyl	Propyl		25.446		38.87			
32*R*	$C(=O)CH(CH_3)_2$	Propyl	Propyl		310.172		−1.97			
32*S*	$C(=O)CH(CH_3)_2$	Propyl	Propyl		27.763		1,961,389			
51*R*	$C(=O)OCH(CH_3)_2$	Propyl	Propyl		408.963		−2.78			
51*S*	$C(=O)OCH(CH_3)_2$	Propyl	Propyl		225.514		3641.98			

(*continued on next page*)

Table 2 (*continued*)

S. no.	R1	R2	R3	Exp BA	Cal BA	CLOGP	Eint	Rank1[a]	Rank2[a]	Rank3[a]
19*R*	CF_3	Propyl	Propyl		43.531		−2.15	B	C	E
19*S*	CF_3	Propyl	Propyl		53.862		−1.73			
30*R*	$C(=O)CF_3$	Propyl	Propyl		44.06		−2.47			
30*S*	$C(=O)CF_3$	Propyl	Propyl		−96.576		−2.56			
31*R*	$C(=O)OCF_3$	Propyl	Propyl		−40.897		−2.63			
31*S*	$C(=O)OCF_3$	Propyl	Propyl		−81.851		427,305.3			
38*R*	CCC	Propyl	Propyl		−236.31		−2.84	B	D	D
38*S*	CCC	Propyl	Propyl		−18.25		−2.8			
34*R*	C(=O)CCC	Propyl	Propyl		−128.1		−2.41			
34*S*	C(=O)CCC	Propyl	Propyl		−436.44		123.65			
21*R*	C(=O)OCCC	Propyl	Propyl		310.042		376,405.8			
21*S*	C(=O)OCCC	Propyl	Propyl		−265.24		295,640.4			
36*R*	CC=C	Propyl	Propyl		227.116		−2.66	A	D	D
36*S*	CC=C	Propyl	Propyl		−14.299		−2.58			
37*R*	C(=O)CC=C	Propyl	Propyl		97.049		−2.19			
37*S*	C(=O)CC=C	Propyl	Propyl		−438.06		4333.18			
7*R*[e]	C(=O)OCC=C	Propyl	Propyl		765[e]		−2.5			
7*S*	C(=O)OCC=C	Propyl	Propyl		−13.15		−2.8			
43*R*	Ph	Propyl	Propyl		176.565		39,842.45	A	G	B
43*S*	Ph	Propyl	Propyl		−9.714		−1.78			
10*R*[e]	C(=O)Ph	Propyl	Propyl		420[e]		−2.7			
10*S*	C(=O)Ph	Propyl	Propyl		−248.94		−3			
9*R*[e]	C(=O)OPh	Propyl	Propyl		330[e]		−3.1			
9*S*	C(=O)OPh	Propyl	Propyl		321.457		−3.1			
48*R*	C=C	Propyl	Propyl		−4.214		−2.57	B	E	A
48*S*	C=C	Propyl	Propyl		14.28		−2.57			
47*R*	C(=O)C=C	Propyl	Propyl		49.407		−2.71			
47*S*	C(=O)C=C	Propyl	Propyl		−170.9		−1.99			
20*R*	C(=O)OC=C	Propyl	Propyl		75.699		−2.84			
20*S*	C(=O)OC=C	Propyl	Propyl		−248.65		1324.52			
45*R*	Bn	Propyl	Propyl		−34.663		39842.45	C	B	A
45*S*	Bn	Propyl	Propyl		−4.788		−1.78			
42*R*	C(=O)Bn	Propyl	Propyl		47.823		−3.58			
42*S*	C(=O)Bn	Propyl	Propyl		59.231		10.11			
5*R*[b]	C(=O)OBn	Propyl	Propyl		279[b]		−3.7			
5*S*[c]	C(=O)OBn	Propyl	Propyl		104[c]		−2.4			
49*R*	Bn	Allyl	Allyl		−159.63		89,4185.6	C	F	F
49*S*	Bn	Allyl	Allyl		77.145		101,681.8			
50*R*	C(=O)Bn	Allyl	Allyl		−222.74		155,968.4			
50*S*	C(=O)Bn	Allyl	Allyl		−138.32		97,202,752			
46*R*	C(=O)OBn	Allyl	Allyl		−110.87		—[d]			
46*S*	C(=O)OBn	Allyl	Allyl		−133.32		22,303.24			
35*RR*(T)	$CH(CH_3)_2$	H	Propyl		−18.286		−2.34			
35*SS*(T)	$CH(CH_3)_2$	Propyl	H		−321.83		2080.05			
35*RS*(CIS)	$CH(CH_3)_2$	Propyl	H		−190.67		−2.46			
35*SR*(CIS)	$CH(CH_3)_2$	H	Propyl		128.6		—[d]			

[a] Vide Table 1.
[b] Experimental *R* enantiomer.
[c] Experimental *S* enantiomer; exp BA, experimental biological activity; cal BA, calculated biological activity; eint, energy of interaction; clogp, calculated *n*-octanol/water partition coefficient
[d] Too high.
[e] Experimental value taken as for *R*.

the compounds as compared to the dipropyl derivatives of the same, except in **49***S*. Further studies need to be undertaken regarding the enhancement of activity due to the presence of alkyl groups at the 3 position and the enhanced activity of the *cis* derivative as compared to the *trans* derivative of a monoalkyl compound. In the only instance of testing the *cis*/*trans* isomers (four isomers of compound **35**), **35***SR*(*cis*) showed an enhanced biological activity of 128.6 (highest amongst the four compounds) but the interaction energy of the receptor–ligand complex could not be calculated signifying that it was highly unstable. On the other hand **35***RS*(*cis*) showed a low calculated biological activity (cal BA) of −190.67 in spite of an energy of interaction (Eint) of

−2.46 (most stable of the four compounds), which also does not support the conclusion. Efforts are currently focussed on establishing these conclusions in a more comprehensive manner and also for the modelling of a more accurate receptor site structure, which has been made difficult due to the presence of various subtypes and presence of more than one site on a single receptor.

In the absence of the knowledge of the 3-D structure of the $GABA_A$ receptor, some recent studies[8,9] have been undertaken using methods like homology modelling to determine the same. Another possible approach towards determination of the structure could be the screening out of compounds with high biological activity acting through a specific site on the receptor structure and modelling the receptor site structure utilising the biological activities of these compounds. 'Pfeiffer's rule' states that more potent the drug the more likely it is to show stereo selectivity due to greater demand for tight receptor binding.[10] Thus higher selectivity on part of the molecules used would lead to a more accurately modelled receptor site in terms of its structural and stereo chemical parameters. Further, stress should also be given to the fact that in case of racemic mixtures resolution of the isomers be carried out before proceeding with biological testing and determination of the more active isomer. It is commonly seen that neglect in terms of stereochemistry often leads to erroneous results.[11] In instances like our own where the activity of the *R* and *S* enantiomers vary greatly, the isomer with lower activity may negate the positive activity of the other isomer present together as a racemic mixture. We feel that these conclusions are of immediate interest to the researchers currently working in this field.

Acknowledgements

The second author is indebted to the Director, Indian Institute of Chemical Biology (Council of Scientific and Industrial Research) for providing with this research opportunity.

References and notes

1. Hadri, A. E.; Abouabdellah, A.; Thomet, U.; Baur, R.; Fortmuller, R.; Siegel, E.; Sieghart, W.; Dodd, R. H. *J. Med. Chem.* **2002**, *45*, 2824.
2. Canney, D. J.; Lu, H. F.; McKeon, A. C.; Yoon, K. W.; Xun, K.; Holland, K. D.; Rothman, S. M.; Ferrendelli, J. A.; Covey, D. F. *Bioorg. Med. Chem.* **1998**, *6*, 43.
3. Williams, K. L.; Tucker, J. B.; White, G.; Weiss, D. S.; Ferrendelli, J. A.; Covey, D. F.; Krause, J. E.; Rothman, S. M. *Mol. Pharmacol.* **1997**, *52*, 114.
4. Klunk, W. E.; Kalman, B. L.; Ferrendelli, J. A.; Covey, D. F. *Mol. Pharmacol.* **1983**, *23*, 511.
5. Holland, K. D.; McKeon, A. C.; Covey, D. F.; Ferrendelli, J. A. *J. Pharmacol. Exp. Ther.* **1990**, *254*, 578.
6. *Cerius*[2], version 4.6 Accelrys, a subsidiary of Pharmacopeia, Inc., San Diego, USA.
7. The activities of the compounds **9**# and **10**# of Table 2 (carbamate and carboxamide derivative with end group Phenyl) have been depicted as of the same order in ref 1.
8. Hosie, A. M.; Smart, T. G. *J. Physiol.* **2003**, 547p.
9. Hosie, A. M.; Dunne, E. L.; Harvey, R. J.; Smart, T. G. *J. Physiol.* **2003**, 547s.
10. Wainer, I. W.; Aboul-Enein, H. Y., Eds. In *The Impact of Stereochemistry on Drug Development and Use*; Chemical Analysis, 142; Wiley Interscience: New York, 1997; P xvii.
11. Wainer, I. W.; Aboul-Enein, H. Y., Eds. *In The Impact of Stereochemistry on Drug Development and Use*; Chemical Analysis, 142; Wiley Interscience: New York, 1997; P xvi.